AMERICAN SOCIETY FOR MICROBIOLOGY | Antimicrobial Agents and Chemotherapy®

EXPERIMENTAL THERAPEUTICS

Polyimidazolium Protects against an Invasive Clinical Isolate of *Salmonella* Typhimurium

Khin K. Z. Mon,[a,b] Zhangyong Si,[c] Mary B. Chan-Park,[c] Linda J. Kenney[a,b]

[a]Mechanobiology Institute, National University of Singapore, Singapore, Singapore
[b]Department of Biochemistry and Molecular Biology, University of Texas Medical Branch, Galveston, Texas, USA
[c]School of Chemical and Biomedical Engineering, Nanyang Technological University, Singapore, Singapore

ABSTRACT Frequent outbreaks of *Salmonella* Typhimurium infection, in both animal and human populations and with the potential for zoonotic transmission, pose a significant threat to the public health sector. The rapid emergence and spread of more invasive multidrug-resistant clinical isolates of *Salmonella* further highlight the need for the development of new drugs with effective broad-spectrum bactericidal activities. The synthesis and evaluation of main-chain cationic polyimidazolium 1 (PIM1) against several Gram-positive and Gram-negative bacteria have previously demonstrated the efficacy profile of PIM1. The present study focuses on the antibacterial and anti-biofilm activities of PIM1 against *Salmonella* in both *in vitro* and *in ovo* settings. *In vitro,* PIM1 exhibited bactericidal activity against three strains of *Salmonella* at a low dosage of 8 μg/mL. The anti-biofilm activity of PIM1 was evident by its elimination of planktonic cells within preformed biofilms in a dose-dependent manner. During the host cell infection process, PIM1 reduces the extracellular bacterial load, which reduces adhesion and invasion to limit the establishment of infection. Once intracellular, *Salmonella* strains were tolerant and protected from PIM1 treatment. In a chicken egg infection model, PIM1 exhibited therapeutic activity for both *Salmonella* strains, using stationary-phase and exponential-phase inocula. Moreover, PIM1 showed a remarkable efficacy against the stationary-phase inocula of drug-resistant *Salmonella* by eliminating the bacterial burden in >50% of the infected chicken egg embryos. Collectively, our results highlight the potential for PIM1 as a replacement therapy for existing antibiotic applications on the poultry farm, given the efficiency and low toxicity profile demonstrated in our agriculturally relevant chicken embryo model.

KEYWORDS polyimidazolium, *Salmonella*, antimicrobial, antibiofilm, chicken egg, CAM

Salmonella enterica serovar Typhimurium (ST) is a Gram-negative bacterium that can cause disease in a broad range of hosts (1). In humans, ST infection can result in both limiting gastrointestinal disease and extraintestinal systemic infection in immunocompromised patients (2–4). Since ST as a pathogen has high zoonotic potential, with human transmission most commonly occurring through a contaminated food chain (5), it raises a major public health concern in the animal and food industries worldwide. The emergence of new, multidrug-resistant (MDR) ST strains (6, 7) further complicates and limits the current antimicrobial therapies available to eradicate this pathogen. *Salmonella* species were listed by the World Health Organization (WHO) among the high-priority antibiotic-resistant bacteria that are in urgent need of new antibiotic development (8, 9). *Salmonella* can exist in either a planktonic form or in a multicellular aggregate form through biofilm production, which allows for prolonged persistence and survival in the host (10). The biofilm state of *Salmonella* is typically antibiotic-tolerant (11, 12), resulting in a chronic bacterial infection that further enhances both the virulence and the transmission rate of the pathogen.

Poultry products are among the highest consumed animal-source products worldwide (13, 14). The consumption of contaminated eggs produced by *Salmonella*-infected layer

Address correspondence to Linda J. Kenney, likenney@utmb.edu.

The authors declare no conflict of interest.

Received 4 May 2022
Returned for modification 5 June 2022
Accepted 15 August 2022
Published 12 September 2022

hens results in foodborne illness, hospitalization, and outbreaks in humans. Therefore, the prevalence of *Salmonella* in the poultry industry not only has a significant economic impact but also poses a major threat to public health. To combat against potential pathogens, as well as to promote poultry growth, antibiotics are commonly incorporated into animal food production (14). However, the excessive use or misuse of antibiotic regimes in poultry production can lead to disastrous outcomes, such as the introduction and spread of multidrug resistant bacteria. Therefore, the development of new therapeutic agents by which to tackle the increasing number of antibiotic-resistant ST isolates and prevent bacterial contamination in the food industry is highly desired.

Exploration into the development of synthetic antimicrobial peptides (AMPs) as alternative therapies to existing antibiotics has gained considerable attention over the years, with some promising results. The number of FDA-approved antimicrobial peptides has been steadily increasing over the past decade (15). Common design principles for AMPs consist of cationic hydrophilic-hydrophobic macromolecules, which enable effective targeting and interaction with negatively charged bacterial cell surfaces to promote a contact-based killing mechanism (16). The binding of AMPs to the microbial envelope leads to increased membrane permeability, structural changes (distortion-disruption), the leakage of cytoplasmic constituents, and eventual bacterial cell death (16–18). Despite its potential for therapeutic usage, there are some limitations associated with the usage of AMPs, including mammalian cell cytotoxicity, discrepancies between *in vitro* versus *in vivo* efficacy, challenges and potency in human administration, difficulty in synthesis, and the high cost of production (19, 20). An alternate antimicrobial compound known as polyimidazolium (PIM) salt has previously demonstrated broad spectrum, potent antimicrobial activity against several Gram-positive and Gram-negative bacteria *in vitro* as well as in a murine infection model (21). The goals of our study were to examine the effectiveness of PIM1 antimicrobial activity against the invasive, multidrug resistant, and hyper-biofilm-forming clinical isolate of *Salmonella* Typhimurium (6), and to compare it to the common strain *Salmonella* Typhimurium 14028s that our lab has used to perform extensive studies in understanding its pathogenesis (22–26). We also employed an agriculturally relevant model, the chicken embryo, to further explore the potential usage of PIM1 for disease prevention and treatment against the prevalence of *Salmonella* in the poultry industry. Overall, PIM1 demonstrated bactericidal activity against clinical isolates of ST under *in vitro* conditions, in a eukaryotic cell infection assay, and in an *in ovo* infection model.

RESULTS

Antibiotic drug panel screening of *Salmonella* Typhimurium strains. A preliminary screening of ST strains against antibiotic drug panels demonstrated high scores for the minimum bactericidal concentration (MBC) assay and half-maximal inhibitory concentration (IC_{50}) value, most notably for the MDR strain (Table 1A and B). Out of 12 antibiotics screened, 8 drugs scored an IC_{50} value higher than 50 μg/mL, attributed to their acquisition of a large multidrug-resistance plasmid (6). The loss of the MDR plasmid in the plasmid-cured strain ΔMDR drastically improved the sensitivity and reduced the score of the MBC assay with antibiotics (Table 1B).

***In vitro* bactericidal activity of PIM1.** The antimicrobial activity of PIM1 was evaluated against ST lab strain 14028s, the multidrug-resistant (MDR) clinical isolate 20081, and the plasmid-cured strain 20081, resulting in the loss of plasmid-encoded antibiotic resistance genes (ΔMDR) *in vitro*. A low minimum inhibitory concentration (MIC) value of 4 μg/mL demonstrated the killing efficacy of the PIM1 polymer against all three *Salmonella* strains (Fig. 1A). The corresponding MBC values where there was no viable bacterial growth detected on the plates were 8 μg/mL for all three strains (Fig. 1A). Therefore, PIM1 displayed potent antimicrobial activity against *Salmonella* Typhimurium isolates at low doses of 4 to 8 μg/mL. To further evaluate the killing kinetics of PIM1, all three strains were grown in the presence of PIM1 at 2× and 4× the MBC value obtained (16 μg/mL and 32 μg/mL). All three *Salmonella* strains were rapidly killed within 15 min at 32 μg/mL, while it took 30 min at 16 μg/mL (Fig. 1B–D). A steady increase in bacterial growth over the same time period was observed in the non-PIM1 treated group, confirming the bacterial killing effect of PIM1 in the treated groups.

TABLE 1 (A) IC_{50} values of *Salmonella* strains screened for 12 antibiotics. (B) MBC assay scores of *Salmonella* strains screened for the same 12 antibiotics

Antibiotics (A)	IC_{50} (μg/mL)		
	14028s	MDR	ΔMDR
Ampicillin	3.498	4026	5.131
Kanamycin	1.473	29.07	2.378
Streptomycin	6.304	5.338	5.356
Carbenicillin	0.6905	167.1	1.499
Gentamicin	0.03811	16.54	3.648
Chloramphenicol	1.845	136.8	5.105
Tetracycline	1.001	58.88	61.73
Trimethoprim	4.583	494.4	14.77
Novobiocin	133.9	152.4	94.73
Spectinomycin	33.35	89.01	40.42
Erythromycin	21.87	26.81	12.52
Nalidixic acid	3.794	350.6	247.2
Antibiotics (B)	**MBC (μg/mL)**		
	14028s	MDR	ΔMDR
Ampicillin	25	6,400	50
Kanamycin	6.25	800	6.25
Streptomycin	25	50	25
Carbenicillin	6.25	400	6.25
Gentamicin	3.125	200	1.56
Chloramphenicol	50	1,600	100
Tetracycline	25	100	100
Trimethoprim	100	3,200	1,600
Novobiocin	1,600	800	1,600
Spectinomycin	6,400	102,400	6,400
Erythromycin	800	800	1,600
Nalidixic acid	12.5	6,400	6,400

PIM1 effects on biofilms. A PIM1 inhibitory effect on *Salmonella* biofilm formation was quantified via a crystal violet assay. In the absence of PIM1, all of the tested bacteria were able to form biofilms under biofilm growth conditions. Specifically, the MDR and ΔMDR strains were observed to have enhanced biofilm thickness, as measured in units of crystal violet absorbance, compared to the lab strain 14028s (Fig. 2A and B). A PIM1 concentration of as low as 16 μg/mL significantly inhibited biofilm formation (Fig. 2A) ($P < 0.0001$ for all three strains). Since the MDR and ΔMDR strains were observed to be hyper-biofilm variants, the ability of PIM1 to effectively eradicate pre-established biofilms was also explored. A dose-dependent effect of PIM1 on biofilm reduction was observed, with a maximal dose of 1,024 μg/mL for all of the tested bacteria (Fig. 2B) ($P < 0.0001$). The effects of PIM1 on biofilm reduction were further confirmed via fluorescence microscopy imaging with SYTO-9 staining (a nucleic acid stain). The *z* axis measurements from the biofilm image stacks validated that the biofilm thicknesses of the MDR and ΔMDR strains were indeed much thicker (~2-fold) than the biofilm of 14028s. For all tested strains, a reduction in biofilm thickness was also evident from the *z* axis scale with post-PIM1 treatment at 1,024 μg/mL (Fig. 3A). All three bacterial strains showed a statistically significant decrease in overall biofilm volume post-PIM1 treatment (Fig. 3B–D) ($P < 0.001$ for 14028s and ΔMDR; $P < 0.05$ for MDR) (see Discussion).

PIM1 reduces adhesion and invasion by extracellular *Salmonella* but does not restrict its intracellular replication. The cytotoxicity of PIM1 on mammalian cells was first assessed with HeLa cells, as this is the common cell line often used for studying the adhesion, replication, and mechanisms of *Salmonella*-host cell interactions during an active infection process (25, 27–29). It was important for us to compare with the wealth of information that we have obtained using HeLa cells in order to examine how the PIM1-treated cells behaved. At the highest concentration of PIM1 (1,024 μg/mL), HeLa cell survival was drastically reduced, with a detection of ~1% viable cells. At lower PIM1 concentrations, the HeLa cell survival rate remained largely unaffected by the PIM1 treatment, with viabilities of 93% (at the MIC), and 83% (at the MBC) (Fig. S1). The half-maximal inhibitory concentration of the drug, also

(A)

PIM1	MIC (μg/ml)			MBC (μg/ml)		
	14028s	MDR	ΔMDR	14028s	MDR	ΔMDR
	4	4	4	8	8	8

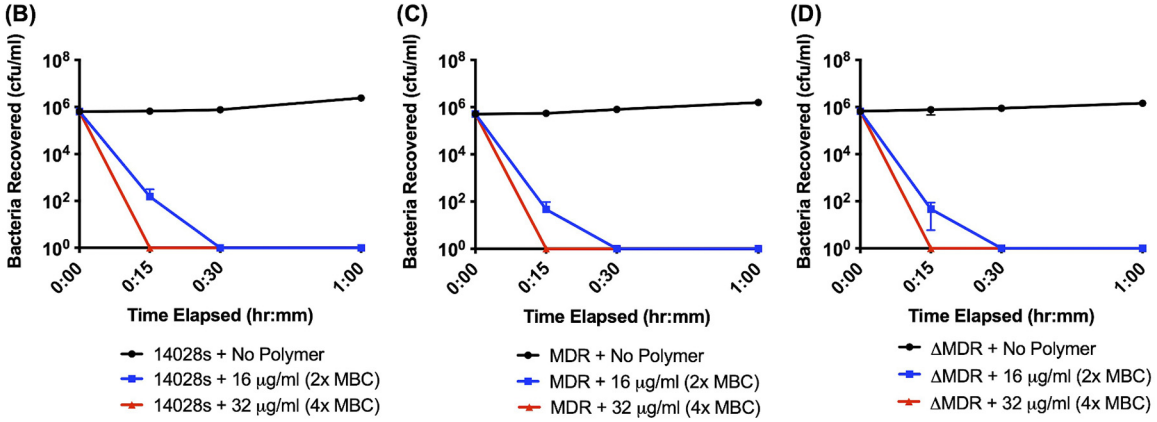

FIG 1 Bactericidal efficiency of PIM1 against three ST isolates. (A) Bacterial cultures in Muller Hinton broth were treated overnight with a PIM1 dose at 2× increments, and the observed minimum inhibitory concentration (MIC) and minimum bactericidal concentration (MBC) for all three strains were recorded. The data are representative of four replicates. (B–D) The bacterial killing kinetics of PIM1 were measured at 2× and 4× concentrations of the MBC value (16 μg/mL and 32 μg/mL) at 15 min, 30 min, and 1 h intervals and compared to the untreated bacterial growth rate. The data plotted were the means of triplicate plate counts of the number of viable bacteria recovered at each time interval. Error bars represent the standard deviation (SD).

known as the IC_{50} value, at which a 50% reduction in HeLa cell viability occurs, was estimated to be 130 μg/mL. Hence, we used PIM1 concentrations (sub-MIC, MIC, and MBC) that were determined not to have a high cytotoxicity effect on HeLa cells for the subsequent *Salmonella* cell infection assay. To examine the effect of PIM1 on the early steps of extracellular *Salmonella* attachment and invasion, PIM1 was added at the same time as the bacterial inoculation. PIM1 exhibited a strong inhibitory activity that reduced the cell adhesion of both the 14028s and MDR strains ($P < 0.0001$) at all tested concentrations compared to the untreated control group (Fig. 4A and B). PIM1 killed extracellular bacteria, effectively blocking adherence to HeLa cells at a sub-MIC treatment level (2 μg/mL) and significantly reducing the total number of attached bacteria by ~10,000-fold for both strains (14028s and MDR). For a *Salmonella* invasion and replication assessment, a gentamicin protection assay was performed to obtain the intracellular bacterial count. Since MDR is a gentamicin-resistant strain, it was replaced with a plasmid-cured MDR strain (ΔMDR) that had lost its gentamicin-resistance phenotype for this assay. In a dose-dependent manner, the presence of PIM1 steadily decreased the number of intracellular *Salmonella* for both the 14028s and ΔMDR strains ($P < 0.0001$) compared to the untreated *Salmonella*-infected HeLa cells (Fig. 4A and B). To assess the ability of PIM1 to target and eliminate intracellular bacteria during an active infection, PIM1 was later added to *Salmonella*-infected HeLa cells, after the gentamicin protection step. At 6 hours postinfection (hpi), the intracellular replication rate of both *Salmonella* strains remained unaffected, even after the PIM1 treatment dosage was incrementally increased (Fig. 4A and B). Taken together, these results indicate that although PIM1 can effectively reduce the extracellular bacteria load, it is unable to target and eradicate intracellular bacteria. PIM1 interference with *Salmonella* infection stages in host cells was further confirmed via confocal fluorescence microscopy at the MIC and MBC levels. A PIM1-fluorescein isothiocyanate (FITC) conjugate was used in the *Salmonella* infections of HeLa cells to visualize and further validate the inhibitory activity of PIM1 during an active infection. Microscopy images corroborated the quantitative colony forming units (CFU) data set, in which a PIM1 treatment was largely effective in visibly reducing the bacterial loads of both strains in a dose-dependent manner (Fig. 4C and D). PIM1-FITC uptake by extracellular *Salmonella* was visualized during the adhesion stage of infection for both strains. However, the PIM1-FITC signal was not

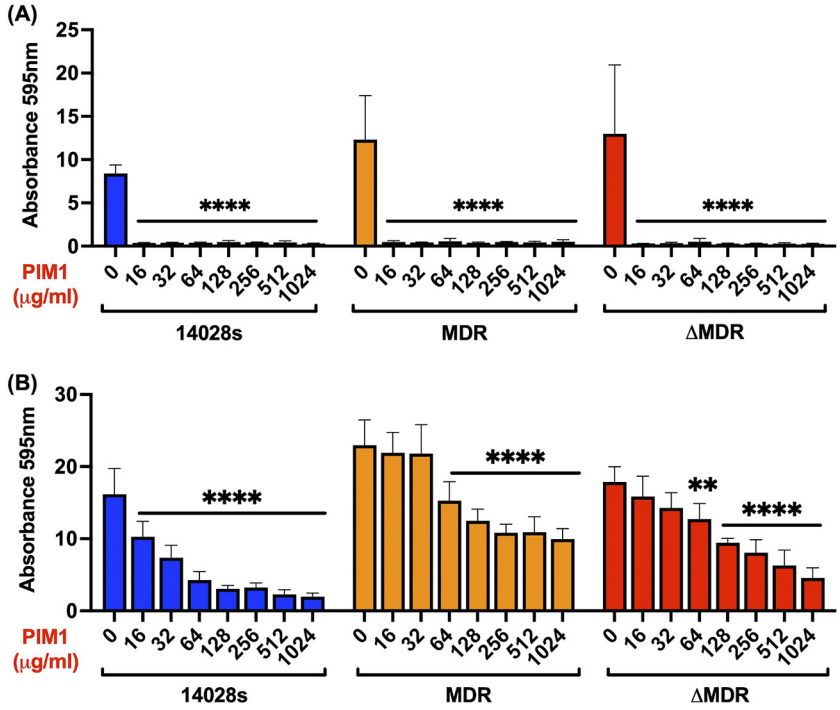

FIG 2 Anti-biofilm activity of PIM1 against three ST strains. (A) PIM1 inhibitory effect on biofilm formation was measured using crystal violet staining for all three strains (14028s, MDR, and ΔMDR) at various concentrations of PIM1. The results represent the mean ± SD (n = 3); ****, $P < 0.0001$ between the untreated and the PIM1-treated groups for all three strains (Dunnett's multiple comparison test). (B) Dose-dependent effects of PIM1 on biofilm degradation as measured by crystal violet staining. The results represent the mean ± SD (n = 3); ****, $P < 0.0001$ between the untreated and all of the PIM1-treated groups for 14028s; ****, $P < 0.0001$ between the untreated and the PIM1-treated groups for MDR, with the exception of the 16 μg/mL and 32 μg/mL PIM1-treated groups (not significant); ****, $P < 0.0001$ between the untreated and PIM1-treated groups for the ΔMDR strains, except for 16 μg/mL (not significant) and 32 μg/mL (**, $P < 0.01$) (Dunnett's multiple comparison test).

detected in intracellular *Salmonella* in either the invasion or the replication stages of infection (Fig. 4C and D).

PIM1 demonstrated therapeutic activity in a chicken egg model of *Salmonella* infection. The ability of PIM1 to control and reduce *Salmonella* colonization in a chicken embryo chorioallantoic membrane (CAM) model at a dosage of 16 μg/egg (2× MBC) was assessed using both stationary-phase and exponential-phase bacterial inocula. The CAM model was comprised of multiple steps and was performed over 12 days from egg incubation to tissue harvesting (Fig. S2). *In ovo* imaging of CAMs infected with mCherry-expressing *Salmonella* 14028s confirmed the signal detection of red fluorescence at the bacterial inoculation site on filter papers. In PIM1-FITC treated CAMs, the red fluorescence bacteria signal was eliminated and replaced by a PIM1 green fluorescence signal at 1 day postinfection (dpi), compared to the untreated CAMs, for both growth-phase inocula (Fig. 5A). Fluorescence *in ovo* images corroborated the significant decrease in bacterial loads in the *Salmonella* 14028s-infected CAMs. With either inoculum, there was a significant reduction in the total bacterial burden recovered from the PIM1-treated 14028s CAMs compared to the untreated 14028s CAMs (Fig. 5B and D) (stationary-phase inoculum: $P < 0.0001$; exponential-phase inoculum: $P < 0.0001$). Furthermore, complete bacterial clearance in both the CAM and the liver was detected in 3 out of 10 chick embryos for the 14028s exponential-phase inocula, post-PIM1 treatment (Fig. 5D). PIM1 also exhibited a potent activity against the MDR strain *in ovo*, with a significant decrease in the bacterial loads for the MDR-infected CAMs (Fig. 5C and E) (stationary-phase inoculum: $P < 0.001$; exponential-phase inoculum: $P < 0.0001$). Notably, a stationary-phase inoculum of MDR was more susceptible to the PIM1 bactericidal effect than was an exponential-phase inoculum. Complete bacterial clearance was detected in 4 out of 7 (>50%) MDR-infected chick embryos with stationary-phase inocula (both CAM

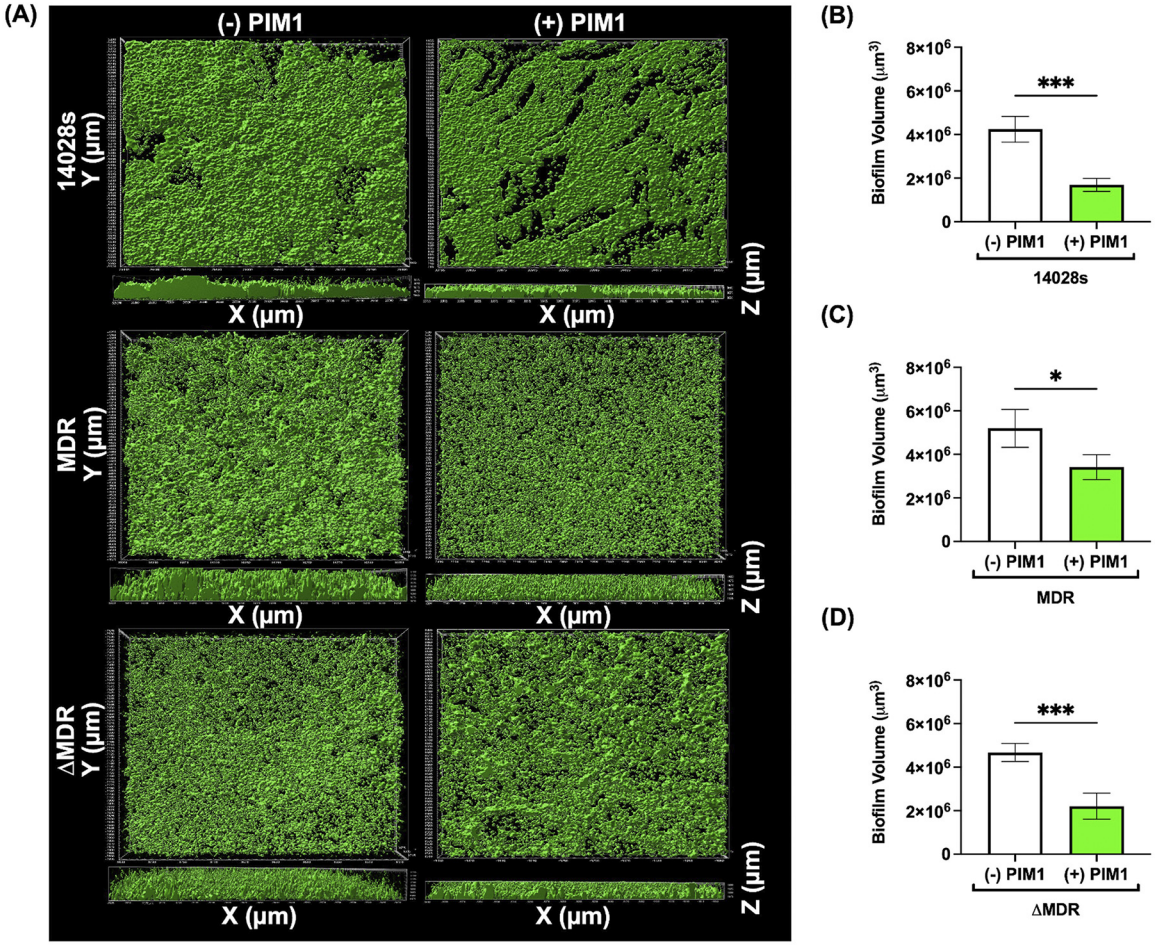

FIG 3 Biofilm degradation capability of PIM1. (A) Three-dimensional modeling of *Salmonella* biofilms stained with SYTO-9 (green) in the absence or presence of 1,024 μg/mL PIM1 using the surface function in Imaris software with the xy-plane and xz-plane views. (B–D) The biofilm volumes for the post-PIM1 treated groups (1,024 μg/mL) for all three strains were significantly reduced in comparison to the untreated groups. The results represent the mean ± SD (n = 2); ***, $P < 0.001$ between the untreated group and the post-PIM1 treated group for the 14028s and ΔMDR strains; *, $P < 0.05$ for the untreated group and the post-PIM1 treated group for the MDR strain (t test).

and liver) (Fig. 5C). Preliminary *Salmonella* infection experiments in the immunodeficient CAM model have indicated that *Salmonella* was capable of rapid dissemination to the internal organ sites of the chicken embryo within 1 hpi. Thus, the ability of PIM1 to limit or reduce the disseminated bacterial load in the liver was also evaluated. A significant reduction of bacteria in the liver was detected, with complete bacterial clearance in 3 out of 10 and in 4 out of 8 livers for the 14028s and MDR strains, respectively (Fig. 5D and E) (exponential-phase inoculum: $P < 0.0001$). For the stationary-phase inoculum, PIM1 treatment exhibited greater efficacy in MDR than in 14028s-infected chick embryos by completely clearing the bacterial burden in 4 out of 7 livers (Fig. 5C) ($P < 0.001$). Although complete bacterial clearance was not detected in the livers of the 14028s-infected chick embryos, there was a significant reduction in the total bacterial burden in the livers, post PIM1 treatment (Fig. 5B) ($P < 0.05$).

DISCUSSION

The emergence and high prevalence of multidrug-resistant bacteria are a global public health threat, as they decrease the effectiveness of conventional antibiotic treatments for pathogen infections. The widespread usage of antibiotics has also led to the natural selection process of microorganisms acquiring multidrug resistance traits or genes, which further complicates the available treatment options (30–32). The development of imidazolium salts as an alternative antimicrobial compound has generated promising results and advances in

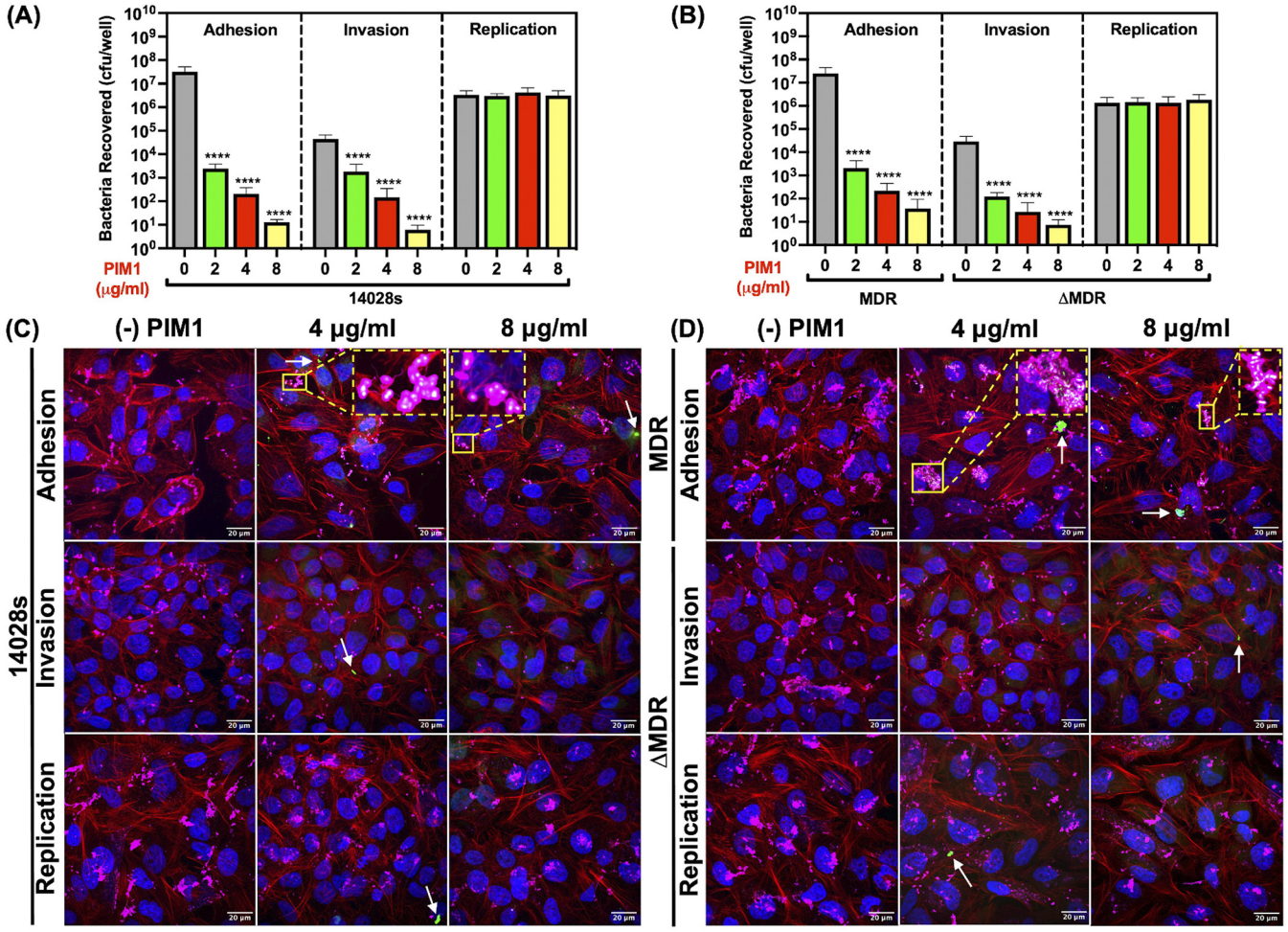

FIG 4 PIM1 targeted and reduced extracellular *Salmonella* during host cell infection. (A) Recovery of *Salmonella* 14028s during adhesion, invasion, and intracellular replication in the presence or absence of PIM1 at sub-MIC, MIC, and MBC concentrations. The results represent the mean ± SD (n = 2); ****, $P < 0.0001$ between the untreated (−) and PIM1-FITC treated groups (2, 4, and 8 μg/mL) (Dunnett's multiple comparison test). (B) CFU assay of *Salmonella* MDR 20081 adhesion, invasion, and replication rates (ΔMDR tested in place of MDR for the gentamicin protection assay) in the presence or absence of PIM1 at MIC and MBC concentrations. The results represent the mean ± SD (n = 2); ****, $P < 0.0001$ between the untreated (−) and PIM1-FITC treated groups (2, 4, and 8 μg/mL) (Dunnett's multiple comparison test). (C) Representative confocal microscopy z stack images of HeLa cells (stained with Hoechst = blue and Phalloadin 568 = red) infected with *Salmonella* 14028s (LPS 647 = magenta) in the absence or presence of PIM1-FITC (green) at MIC and MBC concentrations during different stages of infection. (D) Representative confocal microscopy z stack images of HeLa cells (stained with Hoechst = blue and Phalloidin 568 = red) infected with *Salmonella* MDR and ΔMDR (LPS 647 = magenta) in the absence or presence of PIM1-FITC (green) at MIC and MBC concentrations during different stages of infection. Scale bar = 20 μm. Images showed the colocalization (yellow rectangle and yellow box zoom insert) of PIM1-FITC (green) with extracellular *Salmonella* (magenta) at the adhesion stage of infection. A PIM1-FITC (arrow) signal was also detected outside the cells in the treatment group at the invasion and replication stages of infection, although a colocalization signal of PIM1-FITC with *Salmonella* was not observed.

recent years (33–35). It offers a solution for combating multidrug-resistant bacterial pathogens and bacterial-associated infections. We have previously reported on the potency of a series of main-chain cationic polyimidazolium (PIMs) against several Gram-positive and Gram-negative bacteria (21). In the current study, we demonstrate the efficacy of a selected PIM series, PIM1, against invasive clinical isolates of *Salmonella* Typhimurium 14028s as well as MDR and its plasmid-cured counterpart, ΔMDR.

Under *in vitro* testing conditions with PIM1, bactericidal activity against a planktonic population of *Salmonella* strains was observed with low MIC and MBC scores of 4 to 8 μg/mL. This was identical to the MIC and MBC scores of PIM1 with *Escherichia coli*, another Gram-negative foodborne bacterial pathogen (21). The high sensitivity of the MDR strain toward PIM1 with a low MBC value, as well as its rapid killing kinetics, demonstrated the efficacy of the compound (Fig. 1A and C). The PIM1 mechanism of action on the Gram-negative bacteria *Pseudomonas aeruginosa* has been previously described, and the PIM1 uptake by the bacterial cells was reported to be dependent on the membrane electric potential without disrupting the cell membrane integrity (21).

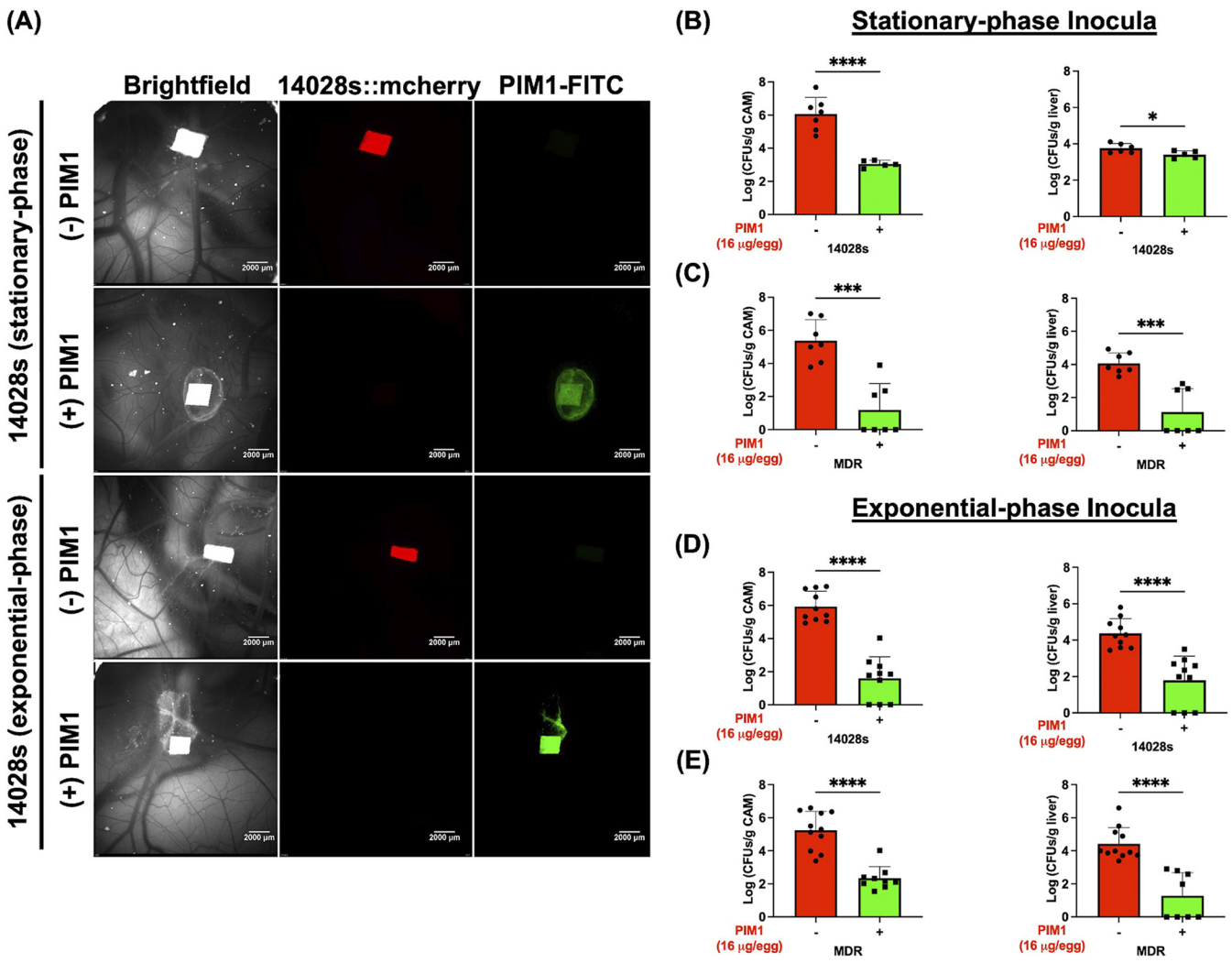

FIG 5 PIM1 reduces *Salmonella* infection in a chicken egg embryo model. (A) Representative live fluorescence stereomicroscope images *in ovo* with *Salmonella* 14028s::mCherry (red) with or without PIM1-FITC (green), 16 μg/egg at 1 dpi, with stationary-phase or exponential-phase inocula. Scale bar = 2,000 μm. (B–E) Quantification of bacteria recovered from the CAMs and livers of chick embryos infected with stationary-phase or exponential-phase inocula of 14028s and MDR in the absence or presence of PIM1 treatment of 16 μg/egg at 1 dpi. The results are presented as the exponential of the CFU, mean ± SD; *, $P < 0.05$; ***, $P < 0.001$; and ****, $P < 0.0001$ between the untreated (−) and PIM1-FITC treated groups (16 μg/egg) (*t* test).

The lifestyle switch from the planktonic state to the biofilm state allows pathogens such as *Salmonella* to survive under harsh environmental conditions and promote chronic carriage as well as the transmission of disease (22, 36). Biofilms are multicellular communities that are embedded in a self-produced matrix of extracellular polymeric substances (EPS) and grow on either biotic or abiotic surfaces that are difficult to eradicate, with a high tolerance toward antimicrobial agents (12, 36, 37). In the current study, the anti-biofilm effect of PIM1 was evident, with the inhibition of biofilm formation being observed at all tested concentrations (Fig. 2A) and with a dose-dependent effect on the reduction of preformed biofilms *in vitro* for all three strains, as measured by a crystal violet assay (Fig. 2B). The inhibitory activity of PIM1 on biofilm formation was found to be a direct consequence of the initial bactericidal effect of PIM1, rather than an active inhibition of biofilm attachment. This was evident from the viable counts of the planktonic bacterial population that were no longer detected in the presence of PIM1. The MDR strain and its plasmid-cured counterpart, ΔMDR, exhibited a hyper-biofilm-forming phenotype compared to that of the lab strain, 14028s. Both of the MDR strains had much thicker biofilms (visible to the naked eye) that were confirmed by a higher absorbance in the crystal violet assay as well as in the *z* axis scales from fluorescence images (Fig. 2A–B and 3A). In addition, the MDR and ΔMDR strains form biofilms at the air-

liquid interface, while the 14028s biofilms are submerged at the bottom of the well. Biofilms that form at the air-liquid interface have been reported to be much thicker and more resistant to cleaning agents (38, 39). Regardless, the PIM1 effectiveness in reducing pre-formed biofilms was evident in terms of reductions in thickness and biofilm volume in dense, three-dimensional architecture images of all *Salmonella* strains, including the hyper-biofilm variants (Fig. 3A–D). The role of PIM1 in reducing biofilm mass was likely exerted through the specific targeting of the detached planktonic fraction of the mature biofilm (a 3-day mature biofilm model was employed in the current study) rather than through the direct disruption of the biofilm matrix. Thus, PIM1 prevented the reformation and reattachment of dispersed bacterial cells to the pre-established biofilm, which explains why PIM1 was unable to completely eradicate the biofilm at the highest tested concentration of 1,024 μg/mL. This high dosage and inability to eradicate the biofilm significantly reduces the therapeutic potential of PIM1 *in vivo*, considering its toxicity issue ($\sim$100% for mammalian cell cytotoxicity at 1,024 μg/mL). However, the use of PIM1 as a potential surface decontamination agent is still worth exploring.

The host infection process by the intracellular pathogen *Salmonella* occurs in different stages: (i) the adhesion or association of bacteria with eukaryotic cells, (ii) host cell invasion, and (iii) intracellular replication. These events can be evaluated *in vitro* based on infection time intervals, a gentamicin protection assay, and a post-gentamicin incubation timeline (40). Therefore, the inhibitory activity of PIM1 on *Salmonella* adhesion, invasion, and replication events were evaluated with some modifications. The attachment of the bacterial pathogen to the host cell surface is the essential first step in the pathogenesis of infection, while the invasion of bacteria into host cells determines the subsequent bacterial survival and establishment of the infection within the host (41). PIM1 interferes early in the bacterial infection process by exhibiting bactericidal activity toward extracellular *Salmonella* strains in a dose-dependent manner. Additionally, at the sub-MIC dosage of 2 μg/mL, at which the PIM1 does not kill the bacteria, the numbers of *Salmonella* that could successfully adhere to and invade the host cells was significantly reduced in the presence of PIM1. In contrast, intracellular *Salmonella* were protected against PIM1 killing during the later stage of the infection process, i.e., replication at 6 hpi (Fig. 4A–D). PIM1-FITC uptake by extracellular *Salmonella* at the adhesion stage of infection was visualized in fluorescence images, further confirming the specificity of PIM1 in targeting against extracellular bacteria (Fig. 4C and D). It is also worth mentioning that the PIM1 concentration used in *Salmonella* cell infection assays was much lower than the IC_{50} cytotoxicity value of the HeLa cells (2, 4, and 8 μg/mL used in the infection assays compared to an IC_{50} of 130 μg/mL). An approximately 16-fold increase in PIM1 concentration would be required for a 50% reduction in HeLa cell viability. Additionally, four other mammalian cell lines have been previously tested, and a much higher IC_{50} concentration ($>$800 μg/mL) was reported (21). These results suggest that PIM1 has targeted bactericidal activity and exhibits minimal cytotoxicity effects toward mammalian cells. Furthermore, the antimicrobial activity of PIM1 at the early stages of the infection process played a crucial role in suppressing bacterial colonization and disrupted the establishment of infection within the host.

Salmonella-associated foodborne outbreaks are often traced back to contaminated eggs or egg-derived products, which serve as an important food vehicle for the transmission of infection (42–44). The positive *in vitro* antimicrobial activity of PIM1 led us to further explore the protective potential of PIM1 administration in a chicken egg model, an agriculturally relevant model for the control of *Salmonella* infection in the poultry industry. The efficiency and susceptibility of antimicrobial treatment are influenced by many factors, including the growth phase of the bacterial inoculum. Stationary-phase bacteria typically exhibit a more resistant phenotype toward antimicrobial agents compared to exponential-phase populations. This is because stationary-phase bacteria undergo changes at both the molecular and cellular levels to withstand harsh environmental conditions (45–47). Hence, PIM1 treatment was tested against infected chicken egg embryos of either stationary-phase or exponential-phase inocula. PIM1 was bactericidal *in ovo*, with a significant reduction in the bacterial load at both the CAM and liver sites (Fig. 5B–E). Such an extraordinary bactericidal effect of

PIM1 was observed after the administration of a low dose (16 μg per egg), irrespective of the inoculum. Since the chicken egg embryo is an immunodeficient model (48), the possibility of triggering host immunity to limit bacterial colonization during a short infection time interval is an unlikely scenario. Instead, the reduction of the bacterial load in the chicken embryo model was most likely a direct consequence of the bactericidal activity of PIM1.

In summary, PIM1 demonstrated potent efficacy against *Salmonella* Typhimurium wild-type 14028s, the multidrug resistant clinical variant MDR, and its ΔMDR derivative. Specifically, PIM1 was effective at a low concentration against planktonic populations. A dose-dependent reduction in biofilms was observed, with the most drastic reduction being observed at the highest concentration tested (1,024 μg/mL). PIM1 interfered with early events during eukaryotic cell infection, further highlighting its ability to target extracellular bacteria to limit pathogen survival and the establishment of infection within the host. The effective antimicrobial activity of PIM1 was consistent in both *in vitro* and *in vivo* settings. In a chicken egg embryo model of *Salmonella* infection, a single, low-dose PIM1 treatment effectively decreased the bacterial load in both the CAM and the liver during infection at 1 dpi. Although PIM1 did not show any evidence of toxicity toward the chick embryos in the current study (at the low administered dose of 16 μg per egg), PIM1 exhibited acute toxicity in mice when administered intraperitoneally at a 6 mg/kg dose (21). A modified derivative of PIM1, PIM1D, which displays reduced hydrophobicity compared to PIM1, resolved the toxicity issue in a murine sepsis infection model. Therefore, the better safety profile of PIM1D suggests a promising therapeutic applicability of the agent as an alternative treatment for poultry associated salmonellosis.

MATERIALS AND METHODS

MIC and MBC of PIM1. Bacterial cultures were prepared in Muller Hinton (MH) broth and incubated overnight at 37°C at 225 rpm. The overnight cultures were resuspended into fresh MH broth (1:100) and incubated at 37°C at 225 rpm to reach the mid-exponential-phase of growth. After incubation, the bacterial cultures were diluted to $\sim 5 \times 10^5$ CFU/mL. The PIM1 polymer was serially diluted in 2-fold increments in MH broth to a concentration ranging from 0 to 64 μg/mL (1 μg/mL = 0.89 μM). Mixed suspensions of the polymer and bacteria were incubated overnight at 37°C without shaking in a 24-well microtiter plate. The MIC was determined with no visible growth of bacteria in a spectrophotometer ($OD_{600\ nm}$). Bacteria without added polymer provided a positive growth control. For the MBC assay, 100 μL of the bacterial-drug mixture suspension from the MIC assay was spread-plated on an LB agar plate and incubated at 37°C overnight. The MBC was recorded as the lowest concentration of polymer that killed 100% of the initial bacterial inoculum.

Killing kinetics of PIM1. Overnight bacterial cultures were resuspended in fresh MH broth (1:100) and incubated at 37°C with shaking at 225 rpm until the cultures reached the mid-exponential phase. The bacterial suspension was then diluted to 1×10^5 CFU/mL in MH broth with a polymer concentration of two or four times the obtained MBC value (16 μg/mL and 32 μg/mL, respectively). A bacterial culture without polymer served as a positive growth control. The bacteria and polymer mixtures were incubated at 37°C at 150 rpm for time intervals of 15 min, 30 min, and 1 h. At each time point, 100 μL of the mixture were serially diluted onto LB agar plates. The number of bacteria recovered were counted after overnight incubation at 37°C. Results in triplicate were averaged and plotted.

Biofilm quantification with crystal violet assay. A crystal violet assay for biofilm quantification in the absence and presence of PIM1 was performed as described previously (22) with some modifications. Briefly, for the biofilm inhibition assay, 2 μL of the overnight culture were inoculated into 198 μL of LB medium without salt and with a serial 2-fold dilution of PIM1 (0, 16, 32, 64, 128, 256, 528, and 1,024 μg/mL) in a 96-well polystyrene plate and grown statically at 30°C for 2 days. For the biofilm degradation assay, the growth medium from pre-established biofilms was removed, washed, and replaced with fresh medium containing a 2-fold serial dilution of PIM1 for a further 24 h of incubation at 30°C. Planktonic cells were then removed, and the attached biofilms in each well were stained with crystal violet. The crystal violet solution was then aspirated, and the wells were washed one time with PBS. This was followed by the addition of absolute ethanol to solubilize the crystal violet. 10-fold dilutions were measured for absorbance at 595 nm using a Bio-Rad plate reader. The experiment was performed twice in quadruplicate for all three strains under each treatment condition.

Fluorescence imaging of biofilms. Biofilms were grown in the μ-slide, 18 wells, glass bottom coverslip (Catalog No. NC1752257, Ibidi) at 30°C for 2 days. Planktonic cells were removed from the well and replaced with fresh growth medium containing 1,024 μg/mL of PIM1. Fresh growth medium only was added into the control wells for the non-treatment group. The μ-slide 18 wells were further incubated at 30°C for 24 h of PIM1 treatment. Each well was then washed and stained with 2 μM SYTO-9 green for a minimum of 30 min before fluorescence images were acquired. Image acquisition was performed using an Olympus Super Res Spinning Disk, SpinSR-10 microscope at 480/500 nm (40× magnification). Image stacks were acquired from seven representative areas of the biofilm surface from each well. The experiment was repeated twice in duplicate for all three strains in the presence or absence of PIM1. Image stacks were reconstructed three-dimensionally, and a biofilm volume analysis was performed using the surface function of Imaris software 9.7.

Mammalian cell cytotoxicity assay. The PIM1 cytotoxicity on the HeLa cells was determined using a 3-[4,5-dimethylthiazol-2-yl]-2,5 diphenyl tetrazolium bromide (MTT) assay. Briefly, the cells were first seeded in

94-well cell-culture plates at a density of 2×10^4 cells per well and incubated at 37°C with 5% CO_2 for 24 h. The cell culture medium was replaced with fresh medium in the presence of PIM1 (at 2, 4, 8, 16, 32, 64, 128, 256, 528, and 1,024 μg/mL) and incubated for a further 24 h. Untreated cells (without PIM1) served as a negative-control, while empty wells with cell medium alone served as a blank control. The next day, the cell medium was aspirated and replaced with fresh medium containing MTT and incubated for 4 h. The MTT solution was then carefully aspirated, and DMSO was added to solubilize. The absorbance readout at 595 nm was recorded using a Bio-Rad plate reader. The percentage of viable cells was calculated using the ratio of the average OD_{595} of treated cells to the average OD_{595} of untreated cells.

Adhesion, invasion, and intracellular survival and replication assays. The ability of PIM1 to interfere with *Salmonella* attachment, invasion, and intracellular replication within HeLa cells during the infection process was investigated with PIM concentrations of the MIC (4 μg/mL), and MBC (8 μg/mL). Briefly, 24-well plates were seeded with 5×10^4 cells/well. *Salmonella* cultures were grown under SPI-1 inducing conditions at the late-log phase and were added to the wells in Dulbecco's modified Eagle's medium (DMEM). The infection assay was carried out as previously described (25) with some modifications. For the adhesion and invasion assay, PIM1 was added to the wells at the same time as the *Salmonella* and was incubated for 30 min after being centrifuged at $500 \times g$ for 10 min. The infection process was stopped for adhesion analysis by lysing the cells with 0.1% Triton X-100 for 10 min, while the invasion analysis was further treated with gentamicin (100 μg/mL) for 1 h to kill the extracellular bacteria before the cells were lysed for plating. Since the MDR strain is resistant to gentamicin, a ΔMDR strain in which the multidrug resistant plasmid was cured from the parent strain (Y. Gao and L.J. Kenney, unpublished results), replaced the MDR strain for both the invasion and the replication assays in which gentamicin treatment was involved. The effect of PIM1 on targeting intracellular bacteria was determined by the addition of PIM1 to the wells after the initial high concentration of the gentamicin (100 μg/mL) treatment for the replication analysis. A lower concentration of gentamicin (20 μg/mL) was added to the untreated group to eliminate extracellular bacterial growth. The infected cells were washed twice with PBS and lysed with 0.1% Triton X-100 for 10 min at 30 min postinfection (adhesion), 1 h post-gentamicin treatment (invasion), and 2 h (replication). The lysates were serially diluted and plated on LB agar to obtain the CFU.

Immunostaining. Immunostaining was carried out on fixed adherent HeLa cells on coverslips at different stages of infection, both in the absence and presence of a PIM1-FITC treatment. Fixed HeLa cells were incubated with primary antibody solution in PBS with 5% bovine serum albumin and 0.1% saponin. *Salmonella* strains were stained with monoclonal rabbit anti-LPS (1:500 dilution). After 1 h, the primary antibody solution was removed, and the cells were gently washed three times with PBS containing 0.1% Tween 20. A secondary antibody solution, which included donkey anti-rabbit 647 (Invitrogen, A-31573), Alexa Fluor phalloidin 568 (Invitrogen A-12380), and Hoechst (Invitrogen, H3570) in a PBS-BSA-saponin buffer was incubated for 1 h at room temperature in the dark. After subsequent wash steps, coverslips containing the adherent stained HeLa cells were inverted onto a microscope slide containing ProLong gold anti-fade reagent (Invitrogen, P36934), sealed with nail polish, and allowed to dry overnight in the dark before image acquisition with an Olympus Super Res Spinning Disk, SpinSR-10 microscope at 100× magnification. Acquired microscopy images were processed with Fiji, in which the background subtraction function was applied in the green channel by taking the mean intensity of the negative-control group.

Chicken egg embryo infection model. Specific pathogen free (SPF) embryonated chicken eggs were purchased from Charles River Laboratories. The chick chorioallantoic membrane (CAM) drops on embryonic development day 3 (ED3) by removing 4 mL of albumin, using a thin needle inserted at the apex of the egg. A small window was made on the top of the eggshell. On ED10, a bacterial inoculum was applied directly onto a small piece of sterile filter paper that was placed on top of the CAM. For the stationary-phase inoculum, an overnight bacterial culture was prepared, whereas a subculture was used for the preparation of the exponential-phase inoculum. PIM1 (16 μg) was then applied on the same spot as the bacterial inoculum deposition site at 1 hpi. At 1 dpi, the CAM layer and the embryo liver were harvested. Samples were then homogenized and serially diluted to determine bacterial numbers via the colony counting method. The imaging of live embryos that were infected with mCherry-tagged ST 14028s was also performed at 1 dpi to detect the fluorescence signal of the bacteria on filter papers, with or without PIM1-FITC treatment, using a Nikon SMZ 18 fluorescence stereomicroscope.

SUPPLEMENTAL MATERIAL

Supplemental material is available online only.

SUPPLEMENTAL FILE 1, PDF file, 0.8 MB.

ACKNOWLEDGMENTS

We thank Stuti Desai for her expertise and guidance with the biofilm aspects of this study and E.P. Greenberg (University of Washington) for his comments on the manuscript. Early studies were supported by a Research Centre of Excellence grant from the Ministry of Education to the Mechanobiology Institute at the National University of Singapore. K.K.Z.M. was supported by CPRT RP200650 to L.J.K., and Z.S. and M.B.C.-P. were funded and supported by the Singapore MOE Tier 3 grant (MOE2018-T3-1-003).

REFERENCES

1. Uzzau S, Brown DJ, Wallis T, Rubino S, Leori G, Bernard S, Casadesús J, Platt DJ, Olsen JE. 2000. Host adapted serotypes of *Salmonella enterica*. Epidemiol Infect 125:229–255. https://doi.org/10.1017/s0950268899004379.
2. Anderson CJ, Kendall MM. 2017. Salmonella enterica serovar Typhimurium strategies for host adaptation. Front Microbiol 8:1983. https://doi.org/10.3389/fmicb.2017.01983.

3. Gordon MA. 2008. Salmonella infections in immunocompromised adults. J Infect 56:413–422. https://doi.org/10.1016/j.jinf.2008.03.012.
4. Acheson D, Hohmann EL. 2001. Nontyphoidal salmonellosis. Clin Infect Dis 32:263–269. https://doi.org/10.1086/318457.
5. Scallan E, Hoekstra RM, Angulo FJ, Tauxe RV, Widdowson M-A, Roy SL, Jones JL, Griffin PM. 2011. Foodborne illness acquired in the United States—major pathogens. Emerg Infect Dis 17:7–15. https://doi.org/10.3201/eid1701.p11101.
6. Mather AE, Phuong TLT, Gao Y, Clare S, Mukhopadhyay S, Goulding DA, Hoang NTD, Tuyen HT, Lan NPH, Thompson CN, Trang NHT, Carrique-Mas J, Tue NT, Campbell JI, Rabaa MA, Thanh DP, Harcourt K, Hoa NT, Trung NV, Schultsz C, Perron GG, Coia JE, Brown DJ, Okoro C, Parkhill J, Thomson NR, Chau NVV, Thwaites GE, Maskell DJ, Dougan G, Kenney LJ, Baker S. 2018. New variant of multidrug-resistant *Salmonella enterica* serovar Typhimurium associated with invasive disease in immunocompromised patients in Vietnam. mBio 9. https://doi.org/10.1128/mBio.01056-18.
7. Wang X, Biswas S, Paudyal N, Pan H, Li X, Fang W, Yue M. 2019. Antibiotic resistance in Salmonella Typhimurium isolates recovered from the food chain through National Antimicrobial Resistance Monitoring System between 1996 and 2016. Front Microbiol 10:985. https://doi.org/10.3389/fmicb.2019.00985.
8. Tacconelli E, Carrara E, Savoldi A, Harbarth S, Mendelson M, Monnet DL, Pulcini C, Kahlmeter G, Kluytmans J, Carmeli Y, Ouellette M, Outterson K, Patel J, Cavaleri M, Cox EM, Houchens CR, Grayson ML, Hansen P, Singh N, Theuretzbacher U, Magrini N. WHO Pathogens Priority List Working Group. 2018. Global priority list of antibiotic-resistant bacteria to guide research, discovery, and development of new antibiotics 7. Lancet Infect Dis 18:318–327. https://doi.org/10.1016/S1473-3099(17)30753-3.
9. WHO. 2017. WHO publishes list of bacteria for which new antibiotics are urgently needed. https://www.who.int/news/item/27-02-2017-who-publishes-list-of-bacteria-for-which-new-antibiotics-are-urgently-needed. Retrieved 7 March 2022.
10. MacKenzie KD, Palmer MB, Köster WL, White AP. 2017. Examining the link between biofilm formation and the ability of pathogenic Salmonella strains to colonize multiple host species. Front Vet Sci 4:138. https://doi.org/10.3389/fvets.2017.00138.
11. MacKenzie KD, Wang Y, Shivak DJ, Wong CS, Hoffman LJL, Lam S, Kröger C, Cameron ADS, Townsend HGG, Köster W, White AP. 2015. Bistable expression of CsgD in Salmonella enterica serovar Typhimurium connects virulence to persistence. Infect Immun 83:2312–2326. https://doi.org/10.1128/IAI.00137-15.
12. González JF, Alberts H, Lee J, Doolittle L, Gunn JS. 2018. Biofilm formation protects Salmonella from the antibiotic ciprofloxacin in vitro and in vivo in the mouse model of chronic carriage. Sci Rep 8:222. https://doi.org/10.1038/s41598-017-18516-2.
13. Products and processing. Gateway to poultry production and products. Food and Agriculture Organization of the United Nations. https://www.fao.org/poultry-production-products/products-processing/en/. Retrieved 7 March 2022.
14. Agyare C, Boamah VE, Osei CNZ, Frank BO. 2018. Antibiotic use in poultry production and its effects on bacterial resistance. Antimicrobial resistance—a global threat. IntechOpen. https://www.intechopen.com/chapters/62553. Retrieved 7 March 2022.
15. Siedenbiedel F, Tiller JC. 2012. Antimicrobial polymers in solution and on surfaces: overview and functional principles. Polymers 4:46–71. https://doi.org/10.3390/polym4010046.
16. Timofeeva L, Kleshcheva N. 2011. Antimicrobial polymers: mechanism of action, factors of activity, and applications. Appl Microbiol Biotechnol 89:475–492. https://doi.org/10.1007/s00253-010-2920-9.
17. Facchi DP, Facchi SP. 2016. N,N,N-trimethyl chitosan and its potential bactericidal activity: current aspects and technological applications. J Infect Dis Ther 4. https://doi.org/10.4172/2332-0877.1000291.
18. Tan H, Ma R, Lin C, Liu Z, Tang T. 2013. Quaternized chitosan as an antimicrobial agent: antimicrobial activity, mechanism of action and biomedical applications in orthopedics. Int J Mol Sci 14:1854–1869. https://doi.org/10.3390/ijms14011854.
19. Ghosh C, Sarkar P, Issa R, Haldar J. 2019. Alternatives to conventional antibiotics in the era of antimicrobial resistance. Trends Microbiol 27:323–338. https://doi.org/10.1016/j.tim.2018.12.010.
20. Mahlapuu M, Håkansson J, Ringstad L, Björn C. 2016. Antimicrobial peptides: an emerging category of therapeutic agents. Front Cell Infect Microbiol 6:194. https://doi.org/10.3389/fcimb.2016.00194.
21. Zhong W, Shi Z, Mahadevegowda SH, Liu B, Zhang K, Koh CH, Ruan L, Chen Y, Zeden MS, Pee CJE, Marimuthu K, De PP, Ng OT, Zhu Y, Chi YR, Hammond PT, Yang L, Gan Y-H, Pethe K, Greenberg EP, Gründling A, Chan-Park MB. 2020. Designer broad-spectrum polyimidazolium antibiotics. Proc Natl Acad Sci U S A 117:31376–31385. https://doi.org/10.1073/pnas.2011024117.
22. Desai SK, Winardhi RS, Periasamy S, Dykas MM, Jie Y, Kenney LJ. 2016. The horizontally-acquired response regulator SsrB drives a Salmonella lifestyle switch by relieving biofilm silencing. Elife 5:e10747. https://doi.org/10.7554/eLife.10747.
23. Desai SK, Padmanabhan A, Harshe S, Zaidel-Bar R, Kenney LJ. 2019. Salmonella biofilms program innate immunity for persistence in Caenorhabditis elegans. Proc Natl Acad Sci U S A 116:12462–12467. https://doi.org/10.1073/pnas.1822018116.
24. Liew ATF, Foo YH, Gao Y, Zangoui P, Singh MK, Gulvady R, Kenney LJ. 2019. Single cell, super-resolution imaging reveals an acid pH-dependent conformational switch in SsrB regulates SPI-2. Elife 8:e45311. https://doi.org/10.7554/eLife.45311.
25. Gao Y, Spahn C, Heilemann M, Kenney LJ. 2018. The pearling transition provides evidence of force-driven endosomal tubulation during Salmonella infection. mBio 9:e01083-18. https://doi.org/10.1128/mBio.01083-18.
26. Singh MK, Kenney LJ. 2021. Super-resolution imaging of bacterial pathogens and visualization of their secreted effectors. FEMS Microbiology Rev 45:fuaa050. https://doi.org/10.1093/femsre/fuaa050.
27. Jones GW, Richardson LA, Uhlman D. 1981. The invasion of HeLa cells by Salmonella typhimurium: reversible and irreversible bacterial attachment and the role of bacterial motility. J Gen Microbiol 127:351–360. https://doi.org/10.1099/00221287-127-2-351.
28. Misselwitz B, Kreibich SK, Rout S, Stecher B, Periaswamy B, Hardt W-D. 2011. Salmonella enterica serovar Typhimurium binds to HeLa cells via Fim-mediated reversible adhesion and irreversible type three secretion system 1-mediated docking. Infect Immun 79:330–341. https://doi.org/10.1128/IAI.00581-10.
29. Khoramian-Falsafi T, Harayama S, Kutsukake K, Pechère JC. 1990. Effect of motility and chemotaxis on the invasion of Salmonella typhimurium into HeLa cells. Microb Pathog 9:47–53. https://doi.org/10.1016/0882-4010(90)90039-s.
30. Blázquez J, Oliver A, Gómez-Gómez J-M. 2002. Mutation and evolution of antibiotic resistance: antibiotics as promoters of antibiotic resistance? Curr Drug Targets 3:345–349. https://doi.org/10.2174/1389450023347579.
31. Mwangi J, Hao X, Lai R, Zhang Z-Y. 2019. Antimicrobial peptides: new hope in the war against multidrug resistance. Zool Res 40:488–505. https://doi.org/10.24272/j.issn.2095-8137.2019.062.
32. Ochoa TJ, Ruiz J, Molina M, del Valle LJOMV, Gil AI, Ecker L, Barletta F, Hall ER, Cleary TG, Lanata CF. 2009. High frequency of antimicrobial resistance of diarrheagenic E. coli in Peruvian infants. Am J Trop Med Hyg 81:296–301. https://doi.org/10.4269/ajtmh.2009.81.296.
33. Demberelnyamba D, Kim K-S, Choi S, Park S-Y, Lee H, Kim C-J, Yoo I-D. 2004. Synthesis and antimicrobial properties of imidazolium and pyrrolidinonium salts. Bioorg Med Chem 12:853–857. https://doi.org/10.1016/j.bmc.2004.01.003.
34. Elshaarawy RFM, Janiak C. 2014. Toward new classes of potent antibiotics: synthesis and antimicrobial activity of novel metallosaldach-imidazolium salts. Eur J Med Chem 75:31–42. https://doi.org/10.1016/j.ejmech.2013.09.029.
35. Valls A, Andreu JJ, Falomir E, Luis SV, Atrián-Blasco E, Mitchell SG, Altava B. 2020. Imidazole and imidazolium antibacterial drugs derived from amino acids. Pharmaceuticals 13:482. https://doi.org/10.3390/ph13120482.
36. Harrell JE, Hahn MM, D'Souza SJ, Vasicek EM, Sandala JL, Gunn JS, McLachlan JB. 2020. Salmonella biofilm formation, chronic infection, and immunity within the intestine and hepatobiliary tract. Front Cell Infect Microbiol 10:624622.
37. Trampari E, Holden ER, Wickham GJ, Ravi A, Martins L de O, Savva GM, Webber MA. 2021. Exposure of Salmonella biofilms to antibiotic concentrations rapidly selects resistance with collateral tradeoffs. NPJ Biofilms Microbiomes 7:3. https://doi.org/10.1038/s41522-020-00178-0.
38. Jha PK, Dallagi H, Richard E, Benezech T, Faille C. 2020. Formation and resistance to cleaning of biofilms at air-liquid-wall interface. Influence of bacterial strain and material. Food Control 118:107384. https://doi.org/10.1016/j.foodcont.2020.107384.
39. Wijman JGE, de Leeuw PPLA, Moezelaar R, Zwietering MH, Abee T. 2007. Air-liquid interface biofilms of Bacillus cereus: formation, sporulation, and dispersion. Appl Environ Microbiol 73:1481–1488. https://doi.org/10.1128/AEM.01781-06.
40. Wu J, Pugh R, Laughlin RC, Andrews-Polymenis H, McClelland M, Bäumler AJ, Adams LG. 2014. High-throughput assay to phenotype Salmonella enterica Typhimurium association, invasion, and replication in macrophages. J Vis Exp 51759.
41. Birhanu BT, Park N-H, Lee S-J, Hossain MA, Park S-C. 2018. Inhibition of Salmonella Typhimurium adhesion, invasion, and intracellular survival via treatment with methyl gallate alone and in combination with marbofloxacin. Vet Res 49:101. https://doi.org/10.1186/s13567-018-0597-8.
42. European Food Safety Authority, European Centre for Disease Prevention and Control. 2021. The European Union One Health 2019 Zoonoses Report. EFS2 19.

43. Festa R, Ambrosio RL, Lamas A, Gratino L, Palmieri G, Franco CM, Cepeda A, Anastasio A. 2021. A study on the antimicrobial and antibiofilm peptide 1018-K6 as potential alternative to antibiotics against food-pathogen Salmonella enterica. Foods 10:1372. https://doi.org/10.3390/foods10061372.
44. Gantois I, Ducatelle R, Pasmans F, Haesebrouck F, Gast R, Humphrey TJ, Van Immerseel F. 2009. Mechanisms of egg contamination by Salmonella enteritidis. FEMS Microbiol Rev 33:718–738. https://doi.org/10.1111/j.1574-6976.2008.00161.x.
45. Agrawal A, Rangarajan N, Weisshaar JC. 2019. Resistance of early stationary phase E. coli to membrane permeabilization by the antimicrobial peptide Cecropin A. Biochim Biophys Acta Biomembr 1861:182990. https://doi.org/10.1016/j.bbamem.2019.05.012.
46. Pletnev P, Osterman I, Sergiev P, Bogdanov A, Dontsova O. 2015. Survival guide: Escherichia coli in the stationary phase. Acta Naturae 7:22–33. https://doi.org/10.32607/20758251-2015-7-4-22-33.
47. Jaishankar J, Srivastava P. 2017. Molecular basis of stationary phase survival and applications. Front Microbiol 8. https://doi.org/10.3389/fmicb.2017.02000.
48. Ribatti D. 2016. The chick embryo chorioallantoic membrane (CAM). A multifaceted experimental model. Mech Dev 141:70–77. https://doi.org/10.1016/j.mod.2016.05.003.